ISSN 2517-7516, Membranes and Membrane Technologies, 2020, Vol. 2, No. 2, pp. 98–108. © Pleiades Publishing, Ltd., 2020.
Russian Text © The Author(s), 2020, published in Membrany i Membrannye Tekhnologii, 2020, Vol. 10, No. 2, pp. 113–124.

Creation of Ion-Selective Membranes from Polyethylene Terephthalate Films Irradiated with Heavy Ions: Critical Parameters of the Process

P. Yu. Apel[a, b, *], I. V. Blonskaya[a], O. M. Ivanov[a], O. V. Kristavchuk[a, b], N. E. Lizunov[a], A. N. Nechaev[a, b], O. L. Orelovich[a], O. A. Polezhaeva[a], and S. N. Dmitriev[a]

[a] *Flerov Laboratory of Nuclear Reactions, Joint Institute for Nuclear Research, Dubna, Moscow oblast, 41980 Russia*
[b] *Dubna State University, Dubna, Moscow oblast, 141980 Russia*
**e-mail: apel@jinr.ru*

Received November 13, 2019; revised November 27, 2019; accepted December 9, 2019

Abstract—A combination of a long exposure to ultraviolet (UV) radiation and the extraction of radiolysis and photolysis products from tracks makes it possible to create ion-selective membranes from polyethylene terephthalate (PET) films irradiated with heavy ions. These membranes exhibit high selectivity for singly charged cations and high transport characteristics in the electrodialysis mode. The aim of this study is to analyze the mechanisms of the transformation of latent tracks into a system of through pores of the subnanometer range in more detail. Polyethylene terephthalate films are irradiated with accelerated Xe and Bi ions with energy losses in the polymer of 11 and 18 keV/nm, respectively. The evolution of the free volume and the accumulation of carboxyl groups in the irradiated films at different stages of the treatment are studied using gravimetry, IR and UV spectroscopy, conductometry, and electron microscopy methods. It is found that the properties of the resulting membranes depend on several critical parameters, which include, in addition to temperature during extraction, the energy loss of the bombarding ion, the pH of the solution used for extraction, and ion fluence. Dramatic changes in the membrane properties are observed at ion fluences at which individual tracks begin to overlap.

Keywords: polyethylene terephthalate, films, accelerated heavy ions, photooxidation, extraction, electrical conductivity, nanopores

DOI: 10.1134/S251775162002002X

1. INTRODUCTION

Track-etched membranes (TMs) produced by the chemical etching of tracks of heavy particles in polymers are well known. The pore size range in TMs extends from 15–20 nm to a few tens of micrometers; therefore, the conventional fields of application of TMs are microfiltration and ultrafiltration. In the past, attempts were made to obtain a finer pore structure by subjecting an ion-irradiated polyethylene terephthalate (PET) film to a softer treatment than chemical etching [1]. Under the action of an aqueous medium under pressure at 100°C, membranes exhibiting a certain ionic selectivity were synthesized; they were used as convenient models, for example, in studying reverse osmosis and nanofiltration mechanisms [2]. However, since these membranes exhibited a low flux in baromembrane processes [1], the studies were not continued. In addition, it was found that organic solvents, such as chloroform and dimethylformamide, dissolve some radiolysis products and PET oligomers and thereby lead to an increase in the free volume in the ion tracks and provide a faster penetration of reactants into the tracks during subsequent etching [3, 4]. Attempts were made to determine the practical applicability of pristine [5] and irradiated films subjected to extraction in the gas separation mode [6, 7]. An increase in the free volume in the vicinity of ion trajectories in the polymer naturally led to an increase in the measured diffusion and gas permeability coefficients. However, the achieved results were of insignificant practical interest because the existing gas separation membranes have significantly better characteristics. Nevertheless, the idea of the nanostructural modification of polymers using heavy ion beams continued to provoke interest among researchers. Thus, many studies were conducted to synthesize ion-conducting membranes by grafting monomers into latent tracks (see, e.g., [8, 9]). Anisotropic proton-conducting membranes with characteristics similar to those of Nafion membranes were synthesized. The transport properties of latent tracks in some commonly used polymers (PET, polycarbonate, polyimide) with respect to aqueous solutions of electrolytes were analyzed in a number of studies by Fink

Table 1. Atomic number, atomic mass, energy, and energy loss of ions used to irradiate a PET film

Ion	Atomic number	Atomic mass, amu	Kinetic energy, MeV	*dE/dx**, keV/nm	Path length, μm
Bi	83	209	710	18	48
Xe	54	132	160	11	20

* Average energy losses of an ion with a given energy in a 12-μm-thick PET film.

et al. [10, 11]. It was shown that, even in relatively hydrophobic polymers, such as those mentioned above, in contact with aqueous solutions, tracks are rapidly saturated with water molecules and act as transport channels for the diffusion of ions into the polymer matrix. The interaction of an irradiated polymer with an electrolyte solution is a fairly complex process, which consists of several stages, which include both diffusion along the tracks and diffusion in the polymer, the swelling of the amorphous regions, and the relaxation processes. As a consequence, a medium that is formally inert with respect to the polymer can have a significant effect on the state of the irradiated polymer, which should be taken into account in practice. For example, the result of asymmetric etching, in which the etching solution contacts only one side of the ion-irradiated film, depends on the type of the neutralizing solution localized on the other side of the polymer film [12]. Reports [10, 11] contributed to a better understanding of the transport of water and ions in ion-irradiated polymer films; however, the authors of those studies focused all their attention on transport directed inside the polymer matrix. The issues concerning the transport of a substance from tracks to the liquid phase were not discussed; however, according to recent studies such as [13–15], this aspect is particularly important in view of the possibility of transforming an ion-irradiated polymer film into a membrane of practical interest. It was found in [13–15] that a combination of a long exposure to ultraviolet (UV) radiation and the extraction of radiolysis and photolysis products from tracks makes it possible to form an array of homogeneous channels with an effective diameter of 0.3–1 nm in PET films irradiated with accelerated heavy ions. Nanochannel walls contain a network of carboxyl groups, whose properties determine the dynamics of ion transport through the channels. In the electrodialysis mode, the fabricated membranes exhibit a high selectivity with respect to singly charged cations and record-breaking transport characteristics. A factor of crucial importance for obtaining this structure is a high level of ion energy loss in the tracks. However, despite the obvious exploitability and promising properties of the fabricated ion-selective membranes, many details of the process of their formation remain unclear. Thus, films from different manufacturers showed completely different results under identical irradiation and extraction conditions. It was also found that depending on extraction temperature, the resulting membranes exhibit the highest flux either with respect to lithium ions or with respect to cesium ions. There is currently significant interest not only in membranes that selectively transfer ions of a certain charge sign, but also in membranes that transfer singly or doubly charged ions and even ions of a particular element [16]. Li-selective membranes [17–20] are of particular importance. These practical aspects have motivated this study, the aim of which is to analyze the mechanisms of transformation of latent tracks of heavy ions into cation-selective through channels in more detail.

2. EXPERIMENTAL

Polymer film. A 12-μm-thick Hostaphan RNK PET film manufactured by Mitsubishi Polyester Films was used as the raw material to fabricate a membrane. According to the manufacturer, the film is prepared by melt coextrusion and consists of an inner layer free from filler particles and thin outer polymer layers containing a small additive of nanodispersed silica. During the manufacturing process, the film is subjected to biaxial stretching and a subsequent heat treatment, which forms the semicrystalline structure of the polymer. The density of the film material is 1.4 g/cm^3. Infrared (IR) spectroscopy studies of the processes that occur during radiolysis and photolysis were conducted using a 175-μm-thick filler-free PET film.

Ion irradiation. PET film samples with a size of 5 × 5 or 10 × 10 cm were irradiated with ^{132}Xe ions on the IC-100 cyclotron and ^{209}Bi ions on the U-400 cyclotron (Flerov Laboratory of Nuclear Reactions, Joint Institute for Nuclear Research). Characteristics of the ions are listed in Table 1. Irradiation was implemented perpendicular to the surface in a vacuum, while varying fluence n in a range of 3×10^9 to 1×10^{12} ion/cm^2. The inhomogeneity of the beam distribution over the target did not exceed ±10%. Specific losses of ions dE/dx were calculated using the SRIM program [21]. It was shown [22] that the program gives overestimated paths of ions with a high atomic number in a target consisting of light elements. Therefore, the dE/dx values in the last but one column of Table 1 represent the result obtained using SRIM and adjusted by a factor of 1.1.

Exposure to UV radiation. Samples of the ion-irradiated films were exposed to UV radiation of LE-30 lamps (Lisma, Saransk, Russia) in air using a pristine PET film as a filter and periodically replacing it with a fresh film. The intensities measured by a TPK-PKM

radiometer were 3–4 W/m^2 in the UVA range (315–400 nm) and ~1 W/m^2 in the UVB range (280–315 nm). The suppression of radiation at a wavelength of <315 nm by a PET filter provided conditions under which photooxidation occurs mostly in tracks and hardly damages the polymer. Thus, the spectral composition of the used radiation was close to that indicated in previous studies (300–450 nm [13–15]).

Gravimetry. Data on the amount of gaseous radiolysis products were obtained according to the weight loss of the samples at ion fluences of 10^9–3×10^{11} cm^{-2}. The 5 × 5 cm samples were weighed on an analytical balance (Mettler Toledo XP205) at least twice before irradiation and twice after irradiation with an interval of a few days to ensure that the values are stable.

Infrared and UV spectroscopy. Infrared spectra were recorded on a Nicolet 6700 Fourier transform IR spectrometer (Thermo Scientific) in the transmission mode at a resolution of 4 cm^{-1}. To eliminate the distortion of the spectra by interference, a thick (175-μm-thick) PET film was used and the sample was tilted relative to the beam direction. Ultraviolet absorption spectra of the PET films before and after irradiation and absorption spectra of aqueous extracts were recorded on an Evolution 600 spectrophotometer (Thermo Scientific) with a spectral slit width of 2 nm.

Extraction of radiolysis and photolysis products. Electrical conductivity of membranes. The extraction of radiolysis and photolysis products from the tracks in the irradiated films was conducted by three methods. In the first case, a 5 × 1 cm sample was placed in 20 mL of water or an electrolyte solution in a glass test tube. The tube was thermostated in a water thermostat for 1–9 hours. The UV absorption spectrum and the pH of the extract were measured. In the second case, a sample with a diameter of 25 mm was placed in a Teflon cell [12] consisting of two compartments and with a hole diameter of 19 mm. Water or an electrolyte solution was poured into the cell, which was then thermostated for a required time; after that, samples of the solution taken from both compartments were subjected to spectrophotometry. Thus, the extraction process was studied under conditions where the film is in a stressed state owing to the thermal expansion of the cell material. In the third case, a round sample with a diameter of 20–25 mm was placed into a cell equipped with two platinum electrodes. The sample was used as a partition between the two compartments of the cell into which an electrolyte solution was poured. The working area of sample S was 0.6 cm^2. The cell was thermostated; the active component of the electrical resistance of the membrane was measured during extraction. An LCR multimeter (HIOKI Instruments, HiTester-3522-50) was used; the meter makes it possible to set a dc or ac voltage across the sample of 0.1–4 V and change the frequency from 1 mHz to 100 kHz. Unlike [13–15], where a strong electric field was used to accelerate extraction from tracks (potential difference at the electrodes of 10 V), in this study, a low voltage (0.5 V) was used to eliminate an uncontrolled heating of the solution in the membrane pores. Upon the completion of extraction, the solution in the cell was replaced with solutions of various salts (KCl, LiCl, $MgCl_2$); further measurements were conducted without removing the sample from the cell. Some of the preliminary experiments were conducted at a frequency of 1333 Hz. Since it is recommended that higher frequencies should be used for an accurate characterization of membranes [23], the "finishing" measurements were conducted at 40 kHz. At this frequency, the resistance of the solution in the cell (without a membrane) was proportional to the resistivity of the solution; it was almost independent of voltage in a range of 0.1–4 V and did not change with a further increase in frequency. To calculate the electrical conductivity of the membrane k_m, the solution resistance R_{sol} was subtracted from the measured resistance of the cell with the membrane R_{meas} and the following well-known formula was used:

$$k_m = \frac{l}{S(R_{meas} - R_{sol})},$$

where l is the membrane thickness.

For extraction at a fixed pH, buffer solutions were used (phosphate and phthalate buffer for a pH of 7 and 4, respectively). The specific electrical conductivities of the buffer solutions with a pH of 4 and 7 were 4.0 and 5.8 mS/cm, respectively, at room temperature. All solutions were prepared using deionized water with a resistivity of 18.2 MΩ cm. Reagents manufactured by Sigma-Aldrich Chemie GmbH—terephthalic acid (TPA), hydroxyterephthalic acid (HTPA), and potassium, lithium and magnesium chlorides—were used.

Electron microscopy. To control the ion fluence in the irradiated films, they were cut into small fragments (≤1 cm^2), which were subsequently subjected to a short chemical etching in an alkaline solution; the density of the formed nanopores was calculated on a Hitachi SU8020 scanning electron microscope (SEM). Owing to the high resolution of the microscope, fluences up to 2×10^{10}–3×10^{10} cm^{-2} were available for direct calculation. In addition, images of membrane cleavages prepared by a technique based on the embrittlement of a polymer matrix by soft photooxidation were examined [24].

3. RESULTS AND DISCUSSION

3.1. Weight Loss during Ion Irradiation

The plot in Fig. 1 shows the decrease in the mass of the 5 × 5 cm samples with an increase in the xenon ion fluence. The linearity of the dependence makes it possible to calculate the mass of the substance removed from one track. It is 4×10^{-16} g. Formally, this mass loss is equivalent to a twofold decrease in the polymer density in a cylinder with a length of 12 μm and a radius

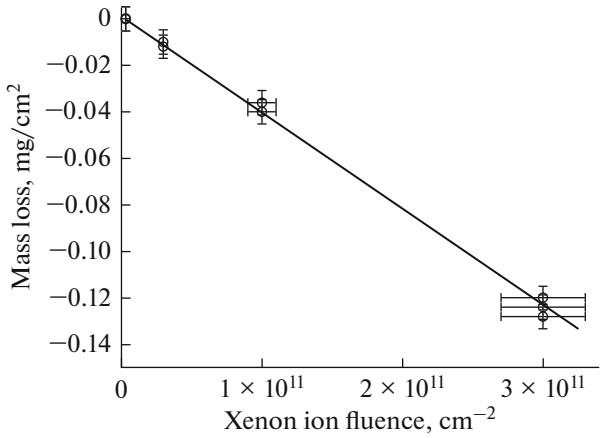

Fig. 1. Variation in the mass of 12-μm-thick PET samples per unit area of the film as a function of xenon ion fluence.

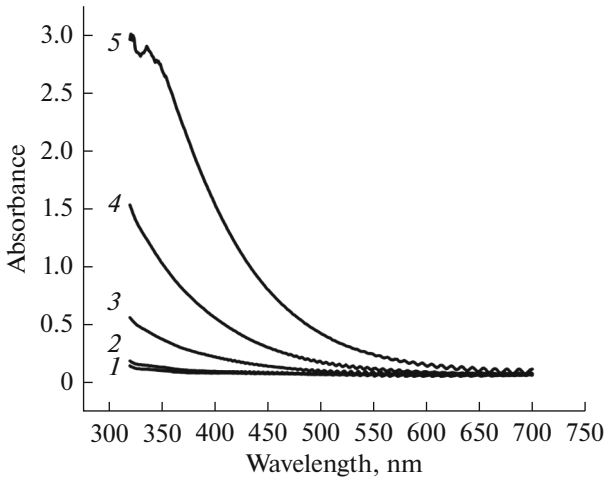

Fig. 2. Optical absorption spectra of (*1*) the pristine 12-μm-thick PET film and the films irradiated with xenon ions. Ion fluence: (*2*) 3×10^9, (*3*) 3×10^{10}, (*4*) 1×10^{11}, and (*5*) 3×10^{11} cm^{-2}.

of 4 nm. This finding correlates well with the track structure revealed by small-angle X-ray scattering [25, 26]. In the cited reports, a latent track in polyimide and polycarbonate is represented as a cylinder with a radius of 3–4 nm, in which the density of the substance is approximately 50% of the initial density. It is known that the main gaseous products of PET radiolysis are carbon monoxide, ethylene, and hydrogen [27]. Assuming for simplicity that they are formed in equal amounts, it is easy to calculate that 1.2×10^7 molecules of gaseous products are released from one xenon ion track and 10^3 molecules leave the polymer matrix per nanometer of track length. It is clear that this factor leads to a significant increase in the free volume in the vicinity of the ion trajectory, that is, in the latent track. The release of a large number of oxygen-containing molecules and hydrogen means that the substance in the track is highly enriched in carbon.

3.2. Photooxidation of Radiolysis Products

Typical optical absorption spectra of ion-irradiated PET samples are shown in Fig. 2. Radiolysis products intensively absorb electromagnetic radiation in the UV region, which is conventionally used in the TM technology to sensitize tracks before chemical etching. The essence of sensitization lies in the photooxidation of structures formed in the core of a heavy ion track. The degradation of these structures is accompanied by a significant decrease in absorption (Fig. 3). Simultaneously, a slight increase in the weight of the irradiated polymer samples is observed; it suggests that oxygen absorption prevails over the cleavage and removal of gaseous photolysis products. Oxygen absorption can primarily indicate the accumulation of carboxyl groups in tracks both in the low-molecular-weight products and at the ends of macromolecules [3, 28]. Despite the fact that the UV spectra of the ion-irradiated films actually cease to change after 30 hours of exposure, twice as much sensitization time (58 hours) was used in further experiments. In this case, the total energy of UV radiation incident on the sample was ~100 J/cm^2, which was approximately equal to that in [13–15].

3.3 Infrared Spectroscopy: Carboxyl Groups

To better understand the essence of the processes that occur in latent tracks at all stages of the transformation of a monolithic PET film into an ion-permeable membrane, IR spectra of the film were measured before and after ion irradiation, after a long UV exposure, and after extraction. Extraction was conducted both immediately after ion irradiation and after sequential exposure of the film to an ion beam and UV radiation. Figure 4 shows fragments of the IR spectra in the vicinity of the band at 3256 cm^{-1}, which is recommended for quantitative determination of the COOH group concentration in PET [29]. During irradiation at a high ion fluence, the absorption of COOH groups significantly increases (spectrum *2*). The subsequent UV exposure leads to a further increase in the carboxyl group content in the sample (spectrum *3*). Spectrum *4* shows a decrease in absorption in the band at 3256 cm^{-1} owing to the removal of some of the COOH groups. Water extraction of radiolysis products from the sample that was not subjected to photooxidation did not lead to detectable changes (spectrum is not shown in Fig. 4). It should therefore be concluded that it is exposure to UV radiation that leads to the formation of water-soluble products in the tracks, whose removal leads to the formation of nanochannels effective for ion transport. The COOH group concentration in the tracks was calculated in accordance with a procedure proposed in [29]. The increase in absorption

in the band at 3256 cm^{-1} corresponds to 1.0×10^6 carboxyl groups per xenon ion track. In these experiments, the ion path was less than the film thickness; thus, each ion transferred the entire kinetic energy of 160 MeV to the polymer. Therefore, the radiation chemical yield of carboxyl groups was ~0.6 per 100 eV of absorbed energy; within the experimental error, this value coincides with the results of [3]. Exposure to UV radiation leads to an increase in the number of carboxyl groups to 1.4×10^6 per track. Subsequent water extraction provides the removal of ~50% of the carboxyl groups formed during photooxidation. Hence, it can be found that the volume concentration of carboxyl groups in the polymer matrix at $n = 10^{11}$ cm^{-2} is about 0.1 mmol/cm^3.

3.4. Ultraviolet Spectra of the Extract: Amount of Substance Removed from the Tracks

A typical absorption spectrum of the extract in the UV region is shown in Fig. 5a. It differs from the spectrum of TPA (Fig. 5b, spectrum *1*) by a stronger absorption in a wavelength region of less than 230 nm and a slowly descending shoulder in a region of >280 nm. It is reasonable to expect that, in addition to TPA, other low-molecular-weight radiolysis and photooxidation products, such as HTPA, benzoic acid, hydroxybenzoic acid [28, 30–32], and aromatic acid esters [33], are present in the tracks. The formation of hydroxy-substituted terephthalate units is quite characteristic of both the radiolytic and photolytic oxidation of PET [31, 32]. In fact, the addition of HTPA to TPA in a ratio of 80 : 20 mol/mol gives spectrum *2* in Fig. 5b, which is much closer to the spectrum of the extract. Taking into account the low specificity of the UV absorption spectra, the presence of other compounds in the extract cannot be ruled out; however, TPA and HTPA are apparently dominant. Chromatographic analysis of water-extracted PET photolysis products suggests that TPA is the main component [34]. The spectra of the TPA photocatalytic oxidation products available in the literature are fairly similar to the spectra of our extracts at a low degree of conversion [35]. It is significant that, for a maximum in the region of ~240 nm, the molar extinction coefficients of these compounds differ only slightly from each other [32, 36]; therefore, the error in the spectrophotometric determination of the number of moles of TPA and TPA analogs associated with the composition uncertainty should be small. The same conclusion can be drawn based on the averaged mass absorption coefficient of PET photolysis products compared with the absorption coefficient of TPA [32].

Figure 6 shows the results of the spectrophotometric determination of the amount of the substance removed from the tracks as a function of water extraction time at 60°C. The points obtained in experiments with samples freely immersed into water lie slightly below the points for rigidly fixed samples. This fact suggests that the mechanical stresses slightly accelerate the release of TPA from the tracks into water; however, the difference hardly goes beyond the limits of error. Within 3 hours, $(2.1 \pm 0.2) \times 10^{-8}$ TPA moles is released from 1 cm^2 of the irradiated film; this

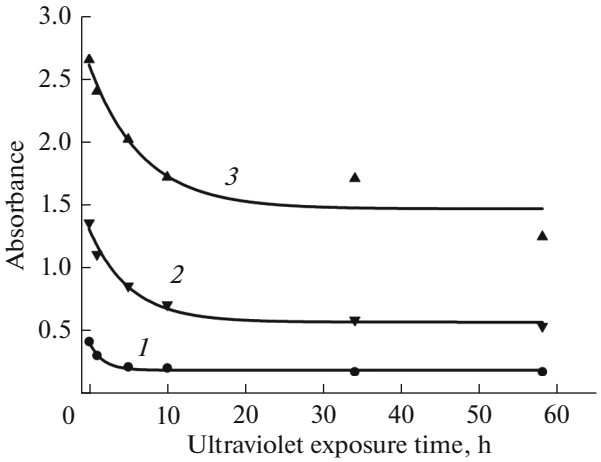

Fig. 3. Decrease in the absorbance of PET films irradiated with xenon ions at a wavelength of 320 nm for fluences of 3×10^{10} and 1×10^{11} cm^{-2} and 350 nm for a fluence of 3×10^{11} cm^{-2} as a function of UV exposure time.

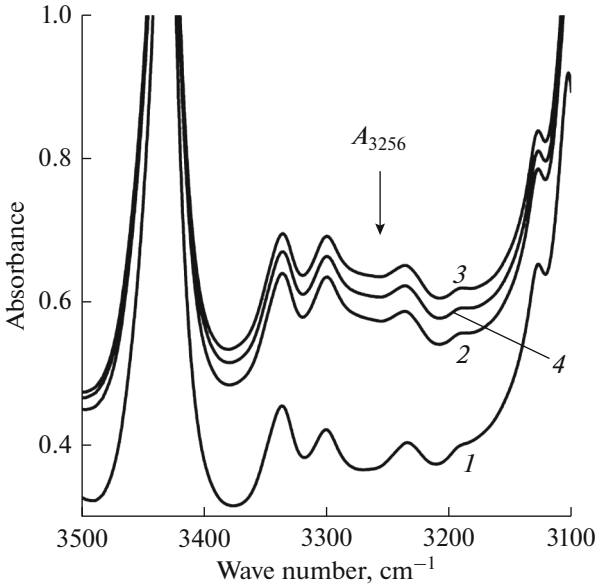

Fig. 4. Infrared spectra of 175-μm-thick PET samples in the vicinity of the absorption band of carboxyl groups: (*1*) the pristine film; (*2*) the film irradiated with Xe ions (7×10^{11} cm^{-2}); (*3*) the film irradiated with Xe ions (7×10^{11} cm^{-2}) and exposed to UV radiation for 58 hours; and (*4*) the film irradiated with Xe ions (7×10^{11} cm^{-2}), exposed to UV radiation for 58 hours, and then subjected to water extraction at 60°C for 9 h. Before recording the spectra, the samples were dried at 105°C.

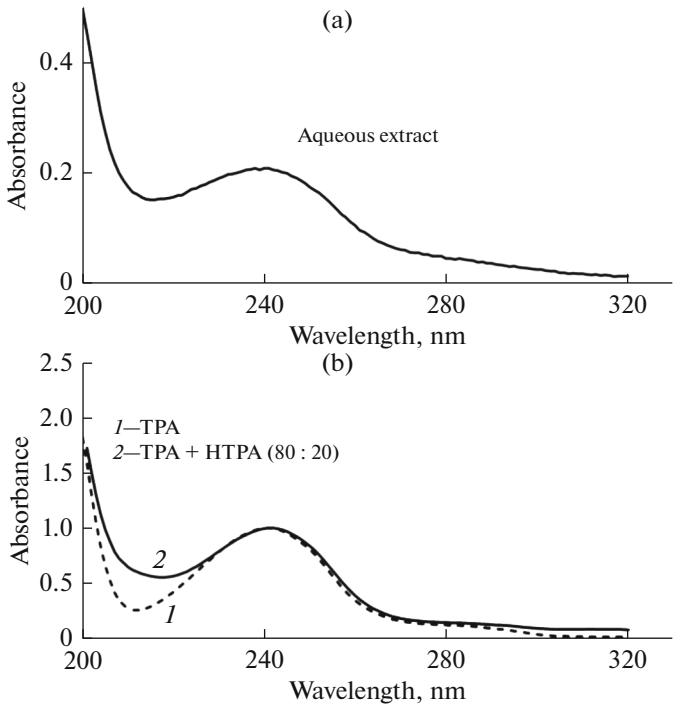

Fig. 5. Absorption spectrum of (a) an aqueous extract from a PET film irradiated with Xe ions (fluence of 7×10^{11} cm^{-2}) and exposed to UV radiation for 58 hours and (b) an aqueous solution of (*1*) TPA and (*2*) a solution of a TPA–HTPA mixture (80 : 20 mol/mol). The spectra in the lower panel are normalized to the absorbance of $A = 1$ at a wavelength of 240 nm.

value corresponds to 10 ± 2 molecules per nanometer of the xenon ion track length. According to reference data on the density of TPA (1.51 g/cm^3), the resulting free volume is formally equivalent to a hollow cylinder with a radius of 0.76 nm. However, it should be emphasized that the estimates of the release of products from the tracks that were made in Sections 3.3 and 3.4 concern only extraction with water, whose pH decreases during extraction. It will be shown in the next section that extraction can be significantly more efficient at a fixed pH.

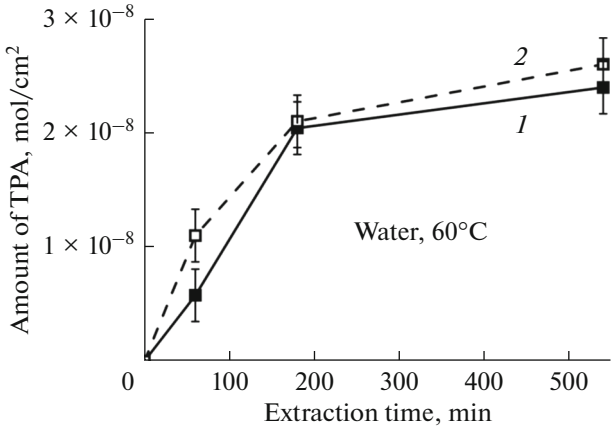

Fig. 6. Number of moles of low-molecular-weight products in terms of TPA extracted with water from 1 cm^2 of a PET film as a function of extraction time at 60°C. The film is irradiated with Xe ions (fluence of 1×10^{11} cm^{-2}) and exposed to UV radiation for 58 hours: (*1*) the sample freely immersed into water and (*2*) the sample rigidly fixed along the perimeter in a Teflon cell.

3.5. Electrical Resistance of Membranes during Extraction: Role of pH

Figure 7a shows typical diagrams of changes in electrical resistance R of a membrane during the extraction of photolysis products from an irradiated PET film. The rate of increase in ionic conductivity drastically increases with temperature. Comparison of the curve for 60°C in Fig. 7a with the dynamics of the release of photolysis products in Fig. 6 suggests that, according to expectations, there is a correlation between the two processes. A characteristic feature of the curves in Fig. 7a is a pronounced kink in the range between 10^5 and 10^6 Ω, which is apparently associated with relaxation processes in the polymer, and the closer the temperature of the medium to the glass transition temperature of PET (80°C), the higher the rate of the relaxation processes. The behavior of electrical resistance reproduces, to a certain extent, the signs of the swelling of an ion-irradiated polymer described in [10, 11]. Repeated experiments conducted under similar conditions showed a poor reproducibility of the results. For an identical temperature, the behaviors of the curves can significantly differ. Analysis of possible

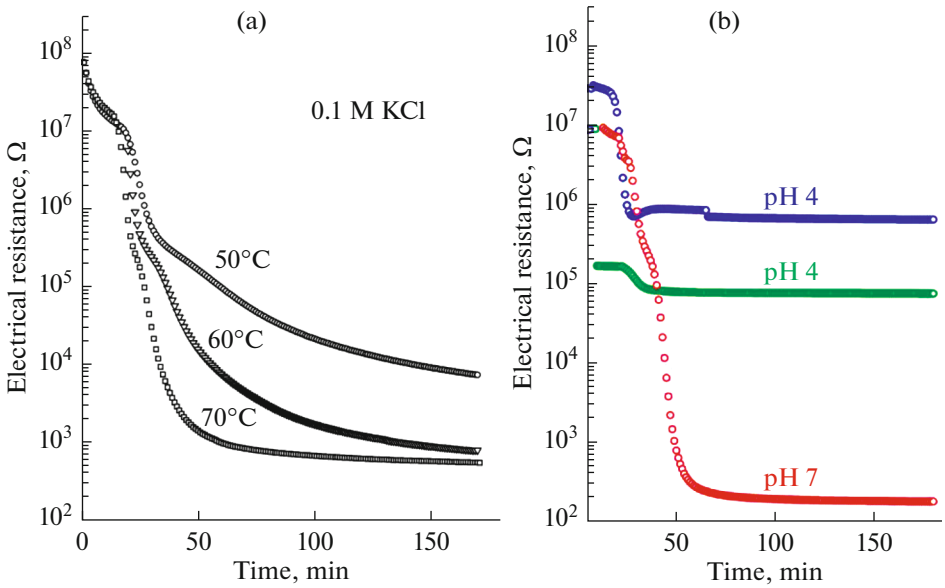

Fig. 7. Electrical resistance of a 12-μm-thick PET film irradiated with Xe ions (1×10^{11} cm^{-2}) and exposed to UV radiation for 58 h as a function of extraction time: (a) extraction in 0.1 M KCl (for the first 20 min, the cell was held at room temperature); at the 20th minute, the cell was placed into a thermostat heated to a given temperature (50, 60, or 70°C); the solution in the cell came to a state close to thermal equilibrium by the 50th minute of the experiment; the resistance of the cell with the solution without a membrane (about 100 Ω) was not subtracted) and (b) extraction in buffer solutions with a pH of 4 and 7 (indicated above the curves) at 60°C.

causes showed that the main source of instability of the behavior of the system is an uncontrolled pH level. During extraction in a small volume of the solution filling the cell, the pH of the solution changes from initial values of 5.6–6.5 to 4.2–4.6. The decrease in pH is caused by the PET photolysis products released into the solution.

In this context, the next set of experiments was conducted at a fixed pH value. Figure 7b shows diagrams of changes in the electrical resistance of the membrane during extraction with buffer solutions with a pH of 4 and 7. Two curves for a pH of 4 exhibit an irregular behavior accompanied by abrupt changes in the membrane current. After 3 hours of treatment, the membrane resistance remains high (10^4–10^5 Ω). In contrast, extraction with a buffer solution with a pH of 7 leads to a rapid and smooth decrease in the resistance, which is reproduced from experiment to experiment. The observed difference between the efficiency of formation of ion-conducting channels at a pH of 4 and 7 is apparently attributed to the fact that the neutral TPA molecule is extracted very slowly, while the rate of extraction in the form of anions is a few orders of magnitude higher. The dissociation of TPA is characterized by constants $pK_{a1} = 3.54$ and $pK_{a2} = 4.46$ [37]. Taking into account the fact that, at a pH of 7, the channel walls contain a large number of dissociated COO^- groups and TPA is a coion, the exclusion of TPA from the solution filling the channel is only natural. It is noteworthy that at the above dissociation constants, a significant portion of TPA molecules should be in the ionic form at a pH of 4. The same is true for carboxyl groups in nanochannels. However, the experiment shows a huge difference in the change in the membrane resistance at a pH of 4 and 7. This behavior of the system can be attributed to the fact that, under limited volume conditions, in particular, in PET nanopores, the acidity of functional groups can significantly decrease compared to the bulk value [38].

3.6. Effect of the Atomic Number of the Ion and Fluence

Experiments showed that a film irradiated with Xe ions at a fluence of 3×10^{11} cm^{-2} does not withstand an elevated-temperature treatment and, typically, disintegrates. Stable results were obtained with samples irradiated with slightly lower doses of Xe and Bi ions ($n \le 10^{11}$ cm^{-2}). Diagrams of change in their electrical resistance R during extraction at a pH of 7 are shown in Fig. 8a. The recorded dependences exhibit extremely strong effects associated with both the level of ion energy loss and the pore density (fluence). Particularly pronounced differences are revealed by comparison of derivatives of the $R(t)$ functions. Thus, at a time of $t =$ 60 min, the dR/dt derivatives for curves *1*, *2*, *3*, and *4* are approximately −2, −7, −150, and −1500 Ω/min, respectively. This behavior suggests that the evolution of the system consists in a deep restructuring of the membrane material (particularly leaching of the low-molecular-weight fraction, swelling, and relaxation of internal stresses in the oriented polymer), rather than

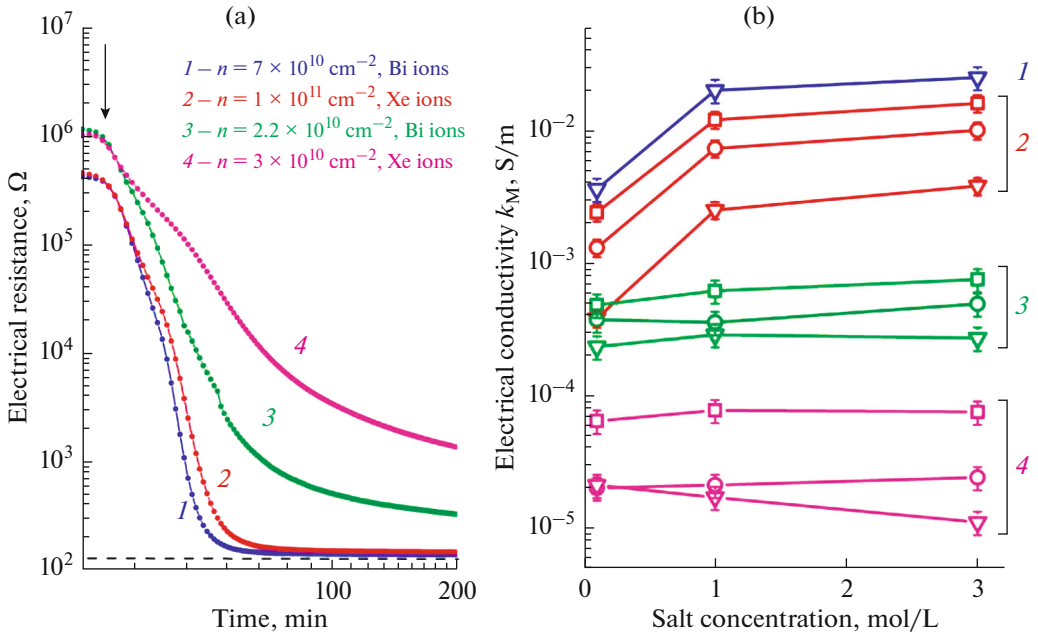

Fig. 8. (a) Electrical resistance of a 12-μm-thick PET film irradiated with Bi ions (curves *1*, *3*) and Xe ions (curves *2*, *4*) and exposed to UV radiation as a function of extraction time in a buffer solution with a pH of 7 at 60°C. Ion fluences are indicated in the figure. The arrow shows the time of immersion of the cell into a thermostat. The dashed line shows the resistance of the cell with the solution without a membrane. (b) Electrical conductivity of the membranes corresponding to curves *1*–*4* in panel (a) measured in □ KCl, ○ LiCl, and ▽ $MgCl_2$ solutions of three different concentrations.

just the diffusion of photolysis products from the pores. The rate of the above processes depends on the size of the radiation damage produced by the ion and the average distance between the pores. Average distance $\langle a \rangle$ between the axes of the nearest neighboring channels is determined by the formula

$$\langle a \rangle = \frac{1}{2\sqrt{n}}.$$

At $n = 10^{11}$ cm^{-2}, the $\langle a \rangle$ value is 17 nm. Taking into account the known data on the track radius [22], it can be concluded that, at this Bi ion fluence, almost the entire polymer is a radiation-modified material. Since crosslinking and degradation in tracks occur simultaneously [6], the polymer is transformed into a three-dimensional network with a low-molecular-weight fraction incorporated into it. It is reasonable to assume that during heating in an aqueous medium and the removal of a low-molecular-weight fraction, this material undergoes shrinkage, which leads to an increase in nanopores. At the same fluence, the conductivity of the material irradiated with Xe ions changes significantly more slowly. This finding is attributed to the smaller track radius, which is approximately proportional to $(dE/dx)^{1/2}$ [22]. Upon switching to fluences of 2×10^{10}–3×10^{10} cm^{-2}, the average distance between the axes of the nearest neighboring tracks increases to ~30 nm. As a consequence, in the case of both Bi and Xe ion tracks, a layer of an intact or slightly damaged polymer (in particular, crystalline phase inclusions) remains between the nearest neighboring channels. In this layer, the swelling/shrinkage rates significantly differ.

Four membranes were prepared by 3-hour extraction, which is shown by dependences in Fig. 8a. After repeated washing of the membranes with deionized water, their electrical resistance in solutions of three different electrolytes was measured (KCl, LiCl, and $MgCl_2$, see Fig. 8b). Membranes 3 and 4 exhibit a behavior that is not observed in the case of conventional TMs with capillary pores: the electrical conductivity is almost independent of the electrolyte solution concentration; in the case of magnesium chloride, it even decreases with an increase in the concentration from 1 to 3 mol/L. A similar behavior, which is caused, for example, by dehydration, is known for ion-exchange membranes [23, 39]. Membrane samples 1 and 2 exhibit an electrical conductivity that is two orders of magnitude higher than that of samples 3 and 4, if membranes synthesized using the same ion are compared in pairs. In both cases, the difference in track density is expressed by a factor of 3. However, this small difference causes a dramatic difference in both the absolute values of electrical conductivity and the behavior of the concentration dependence of the conductivity. The behavior of the concentration dependence of the electrical conductivity of membranes 1 and 2 is close to that of conventional TMs whose pore radius is comparable to the thickness of the electric double layer [40].

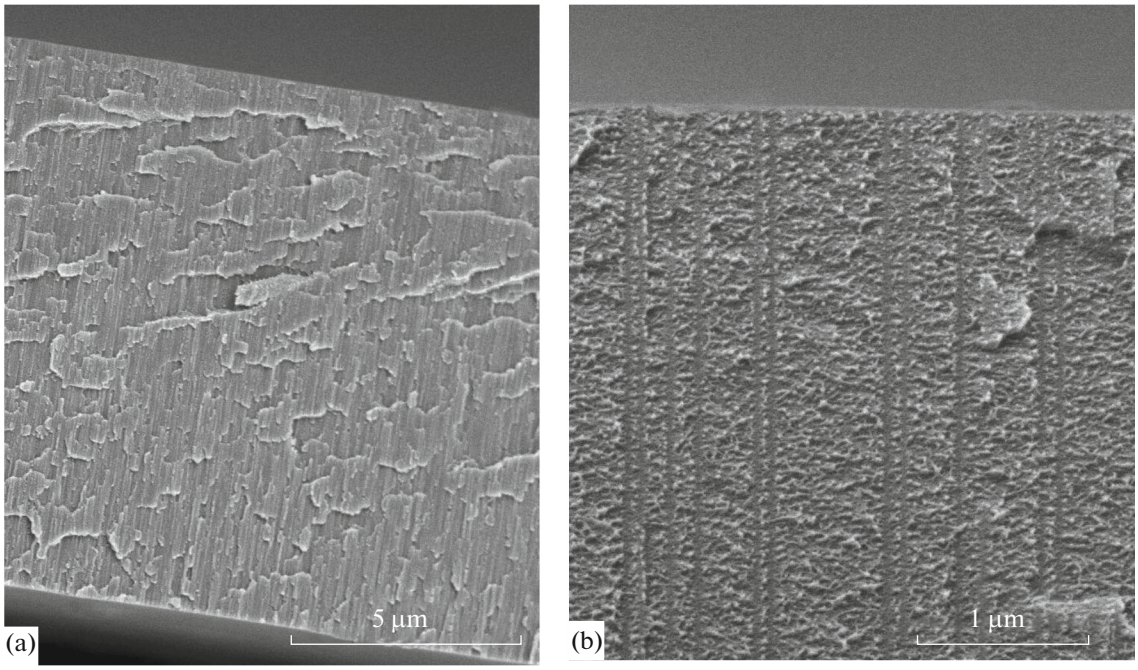

Fig. 9. Electron microscopic images of fractures of a PET film irradiated with xenon ions and subjected to a long UV exposure. The ion fluence is (a) 3×10^{11} and (b) 3×10^{9} cm^{-2}.

3.7. Membrane Structure according to SEM

Figure 9 shows electron micrographs of fractures of the fabricated membranes. The image on the left corresponds to a membrane with a track density of 3×10^{11} per square centimeter. The array of closely spaced parallel channels forms a highly anisotropic structure piercing the entire film from one side to the other. The image on the right shows a membrane with a track density of 3×10^{9} cm^{-2} at a higher magnification. Distinct channels with a diameter of 20–30 nm are clearly visible on the cleaved surface. The membrane fractures look identical before and after extraction. Outside the channels, the fracture surface consists of alternating light and dark areas. The light grains with a size of 5–20 nm are PET crystallites. It is known that PET films manufactured by the conventional biaxial stretching method and subsequent heat treatment have a semicrystalline structure. The sizes of the crystalline and amorphous regions determined by X-ray scattering, transmission microscopy, and atomic force microscopy [41, 42] correspond to the scales of the grain structure elements observed on the transverse fractures. The transverse size of the channels that do not have a grain structure correlates well with the radius of the low-density zone in xenon ion tracks (13 nm) calculated from small-angle X-ray scattering data under the assumption of a homogeneous channel structure [43]. Hence, an ion passing through the polymer destroys the crystallites in the immediate vicinity of the ion trajectory; as a result, the channels of the tracks look like gray homogeneous entities. Upon the embrittlement of PET by soft UV radiation, photooxidative degradation is localized in the amorphous regions of the polymer and does not destroy crystallites. The used embrittlement technique therefore made it possible to recognize latent tracks against the background of a semicrystalline polymer matrix.

The authors of [13–15] concluded that cations are transported along a narrow hollow core of a track with a diameter of about 1 nm. The images recorded by us neither confirm nor refute the existence of this core. The SEM resolution provides a reliable observation of etched hollow channels with a diameter of ~10 nm [12]; however, an object smaller by an order of magnitude cannot be observed using this technique.

CONCLUSIONS AND FURTHER RESEARCH

Thus, ion-conducting channels formed by ion irradiation and subsequent photooxidation and extraction are amorphized regions threaded by a three-dimensional network and characterized by a low density and a high content of terminal carboxyl groups. The presence of a hollow core with charged walls remains debatable. Useful information about the radius of the channel along which ions are transported can be obtained by studying the anisotropy of the electrical resistance of the membrane. If the radius of the ion-conducting channel is 10 nm, then, at a pore density of 10^{11} cm^{-2}, the average distance between the axes of the nearest neighboring channels is less than two radii and the membrane should exhibit ionic conductivity not

only in the transverse direction, but also in the longitudinal direction (parallel to the surface). If the radius of the transport channel is an order of magnitude smaller, then, even at a fluence of 10^{11} cm^{-2}, the membrane should be highly anisotropic. The degree of anisotropy should be measured in future studies. In addition, it is necessary to use more advanced membrane resistance measurement methods than the difference methods used in this work [39]. Diffusion potential measurements to determine the selectivity and membrane testing in the electrodialysis mode will be performed at the next stages of the study.

Conventional PET TMs hardly swell in aqueous solutions; the gel phase in the form of a thin surface layer resulting from contact with water affects transport properties only in the case of small pore sizes [40]. The samples obtained in this study, conversely, showed a significant change in their properties during water saturation. Accordingly, the gel phase is an important component of the structure; therefore, it appears reasonable to study membranes of this type in terms of recently developed microheterogeneous models [44].

The obvious fact that ion transport through the initially monolithic PET film becomes possible owing to the formed free volume requires an additional brief comment. Our studies have shown that the most significant contribution to the formation of the free volume comes from heavy ion bombardment. However, ionic conductivity remains very low. It increases significantly after UV exposure, which does not increase free volume at all. Evidently, ion tracks themselves are extremely hydrophobic. Their hydrophilization by photooxidation opens the gate to the diffusion of water and the motion of ions. Extraction of low-molecular-weight photooxidation products completes the formation of a hydrophilic channel.

Our study has made it possible to determine some critical parameters of the transformation of a latent track into a channel exhibiting a high ionic conductivity. First, by setting the pH of the medium used for extraction, it is possible to effectively control the rate and degree of removal of photolysis products from the tracks. Second, ion energy losses play a significant role; they are responsible for the transverse size of the damage. A 1.6-fold difference in energy losses leads to an order of magnitude difference in membrane conductivity. The third parameter—ion fluence—in combination with the second parameter determines the boundary where the transport properties of the resulting membranes abruptly change owing to the merging of the neighboring tracks.

ACKNOWLEDGMENTS

The authors thank N.S. Kirilkin for his assistance in irradiating the samples with Bi ions. P.Yu.A. thanks Feng Liu for useful discussions.

REFERENCES

1. V. V. Berezkin, A. N. Nechaev, S. V. Fomichev, B. V. Mchedlishvili, and N. I. Zhitaryuk, Colloid J. USSR, Plenum Publishing, **53**, 292 (1991).
2. A. E. Yaroshchuk, Adv. Colloid Interface Sci. **60**, 1 (1995).
3. P. Yu. Apel' and L. I. Kravets, Khim. Vys. Energ. **25**, 138 (1991).
4. P. Yu. Apel' and L. I. Kravets, Khim. Vys. Energ. **26**, 295 (1992).
5. K. Schaupert, D. Albrecht, P. Armbruster, and R. Spohr, Appl. Phys. **44**, 347 (1987).
6. P. Yu. Apel, N. Angert, W. Bruechle, H. Hermann, U. Kampschulte, P. Klein, L. I. Kravets, Yu. Ts. Oganessian, G. Remmert, R. Spohr, T. Steckenreiter, C. Trautmann, and J. Vetter, Nucl. Instrum. Methods Phys. Res. **86**, 325 (1994).
7. M. Esser, P. Yu. Apel, W. Bruechle, J. Furmann, B. Heinrich, G. Remmert, R. Spohr, C. Trautmann, and J. Vetter, Nucl. Instrum. Methods Phys. Res. **91**, 157 (1994).
8. N. Betz, Nucl. Instrum. Methods in Phys. Res. **55**, 105 (1995).
9. Y. Kimura, J. Chen, M. Asano, Y. Maekawa, R. Katakai, and M. Yoshida, Nucl. Instrum. Methods in Phys. Res. **263**, 463 (2007).
10. *Heavy Ion Physics: VI Intern. School-Seminar, Dubna, Russia (22–27 September, 1997*), Ed. by Fink D., Ghosh S., Hirata K., Klett R., Dwivedi K.K., Vacik J., and Hnatowicz V. (World Scientific, Singapore, 1998).
11. D. Fink, A. Petrov, M. Muller, T. Asmus, V. Hnatowicz, J. Vacik, and J. Cervena, Surf. Coat. Technol. **158–159**, 228 (2002).
12. P. Y. Apel, V. V. Bashevoy, I. V. Blonskaya, N. I. Lizunov, O. L. Orelovitch, and C. Trautmann, Phys. Chem. Chem. Phys. **18**, 25421 (2016).
13. Q. Wen, D. Yan, F. Liu, M. Wang, Y. Ling, P. Wang, P. Kluth, D. Schauries, C. Trautmann, P. Apel, W. Guo, G. Xiao, J. Liu, J. Xue, Y. Wang, Adv. Funct. Mater **26**, 5796 (2016).
14. P. Wang, M. Wang, F. Liu, S. Ding, X. Wang, G. Du, J. Liu, P. Apel, P. Kluth, C. Trautmann, and Y. Wang, Nat. Commun. **9**, 569 (2018).
15. P. Wang, X. Wang, Y. Ling, M. Wang, S. Ding, W. Shen, Z. Wang, Y. Wang, F. Liu, Radiat. Meas. **119**, 80 (2018).
16. P. Yu. Apel, O. V. Bobreshova, A. V. Volkov, V. V. Volkov, V. V. Nikonenko, I. A. Stenina, A. N. Filippov, Yu. P. Yampolskii, and A. B. Yaroslavtsev, Membr. Membr. Technol. **1**, 45 (2019).
17. S. E. Kesler, P. W. Gruber, P. A. Medina, G. A. Keoleian, M. P. Everson, and T. J. Wallington, Ore Geol. Rev. **48**, 55 (2012).
18. T. Hoshino, Fusion Eng. Des. **88**, 2956 (2013).
19. A. Somrani, A. H. Hamzaoui, and M. Pontie, Desalination **317**, 184 (2013).
20. X.-Y. Nie, S.-Y. Sun, Z. Sun, X. Song, J.-G. Yu, Desalination **403**, 128 (2017).
21. J. F. Ziegler, J. P. Biersack, and U. Littmark, *The Stopping and Range of Ions in Solids* (Pergamon: New York, 1985). http://www.srim.org.

22. P. Yu. Apel, A. Schulz, R. Spohr, C. Trautmann, V. Vutsadakis, Nucl. Instrum. Methods Phys. Res. **146**, 468 (1998).
23. N. Berezina, N. Gnusin, O. Dyomina, and S. Timofeev, J. Membr. Sci. **86**, 207 (1994).
24. O. L. Orelovitch, P. Yu. Apel, and B. Sartowska, J. Microscopy **224**, 100 (2006).
25. S. Abu Saleh and Y. Eyal, Appl. Phys. Lett. **85**, 2529 (2004).
26. S. Abu Saleh and Y. Eyal, Nucl. Instrum. Methods Phys. Res. B. **236**, 81 (2005).
27. D. K. Avasthi, J. P. Singh, A. Biswas, and S. K. Bose, Nucl. Instrum. Methods Phys. Res. **146**, 504 (1998).
28. T. Grossetete, A. Rivaton, J. L. Gardette, C. E. Hoyle, M. Ziemer, D. R. Fagerburg, and H. Clauberg, Polymer **41**, 3541 (2000).
29. R. L. Addleman and V. I. J. Zichy, Polymer **13**, 391 (1972).
30. T. Steckenreiter, E. Balanzat, H. Fuess, and C. Trautmann, Nucl. Instrum. Methods Phys. Res. **131**, 159 (1997).
31. X. Fang and G. Mark, and C. von Sonntag, Ultrason. Sonochem. **3**, 57 (1996).
32. S. Krishnan, S. B. Mitra, P. M. Russell, and G. Benz, ACS Symp. Ser. **287**, 389.
33. R. Buchalla and T. H. Begley, Radiat. Phys. Chem. **75**, 129 (2006).
34. A. I. Vilensky, D. L. Zagorsky, V. Ya. Kabanov, and B. V. Mchedlishvili, Radiat. Meas. **36**, 131 (2003).
35. A. Shafaei, M. Nikazar, and M. Arami, Desalination **252**, 8 (2010).
36. D. Doub and J. M. Vandenbelt, J. Am. Chem. Soc. **69**, 2714 (1947).
37. *Chemist's Handbook*, Ed. by Nikol'skii B.P. (Khimiya, Moscow, 1964) [in Russian].
38. C. Sanborn, J. V. Chacko, M. Digman, and S. Ardo, Chem. **5**, 1648 (2019).
39. *Membranes and Membrane Technologies*, Ed. by Yaroslavtsev A.B. (Nauchnyi Mir, Moscow, 2013) [in Russian].
40. V. V. Berezkin, O. A. Kiseleva, A. N. Nechaev, V. D. Sobolev, N. V. Churaev, Kolloid. Zh. **56**, 319 (1994).
41. H. Chang, J. M. Schultz, and R. M. Gohil, J. Macromol. Sci. **32**, 99 (1994).
42. F. Dinelli, H. E. Assender, K. Kirov, and O. V. Kolosov, Polymer **41**, 4285 (2000).
43. D. I. Svergun, A. B. Semenyuk, L. Yu. Mogilevskii, V. V. Berezkin, A. N. Nechaev, and B. V. Mchedlishvili, Kolloidn. Zh. **53**, 143 (1991).
44. V. S. Nichka, S. A. Mareev, M. V. Porozhnyy, S. A. Shkirskaya, E. Yu. Safronova, N. D. Pismenskaya, and V. V. Nikonenko, Membr. Membr. Techn. **1**, 190 (2019).

Translated by M. Timoshinina